**Algal Research-biomass Biofuels And Bioproducts**
March 2020, Volume 46 Pages 101783 (11p.)
https://doi.org/10.1016/j.algal.2019.101783
https://archimer.ifremer.fr/doc/00865/97736/



# Impact of ocean acidification on the metabolome of the brown macroalgae *Lobophora rosacea* from New Caledonia

Gaubert Julie [1, 2, *], Rodolfo-Metalpa Riccardo [2], Greff Stephane [3], Thomas Olivier P. [4], Payri Claude E. [2]

[1] Sorbonne Universités, Collège Doctoral, F-75005 Paris, France
[2] UMR ENTROPIE (IRD, UR, CNRS), Institut de Recherche pour le Développement, B.P. A5, 98848 Nouméa Cedex, New Caledonia
[3] Institut Méditerranéen de Biodiversité et d'Ecologie Marine et Continentale (IMBE), UMR 7263 CNRS, IRD, Aix Marseille Université, Avignon Université, Station Marine d'Endoume, rue de la Batterie des Lions, 13007 Marseille, France
[4] Marine Biodiscovery, School of Chemistry and Ryan Institute, National University of Ireland Galway (NUI Galway), University Road, H91 TK33 Galway, Ireland

* Corresponding author : Julie Gaubert, email address : julieg1907@gmail.com

**Abstract :**

Macroalgae are critical components of coral reef ecosystems. Yet, they compete for space with corals, and in case of environmental disturbances, they are increasingly involved in phase-shifts from coral-dominated to macroalgae-dominated reefs. As regard to climate change, ocean acidification (OA) has been shown to be detrimental to corals and could favor macroalgal proliferations. However, little is known about the effects of OA on macroalgal phenotypes. Comparative metabolomic studies are particularly relevant to assess phenotypic responses of macroalgae to stress as some seaweed are known to produce a large diversity of specialized metabolites involved in various ecological functions. The main aim of our study was to explore the impact of OA on the metabolome of brown macroalgae using Lobophora rosacea as a model species. This species is widespread in New Caledonian lagoons where it is a key component of coral-algal interactions. Metabolomic changes were analyzed using Liquid Chromatography-Mass Spectrometry (UPLC-HRMS) applied to three different OA scenarii: low and variable pH over a long-term timescale (in situ at Bourake), low and constant pH over a short-term timescale (ex situ experiment), and current pH (control). Different metabotypes were defined in diverse pH conditions, and a significant decrease in some specialized metabolites concentrations was noticed at low pH including lobophorenols B and C as well as other oxylipin derivatives. We suggest a down-regulation of metabolic pathways involving lobophorenols, in low pH conditions, or their transformation, which is in accordance with the optimal defense theory. In addition, we used Microtox (R) bioassays as a proxy for macroalgal toxicity and found no significant differences between low pH and control samples. This study details the first metabolomic-based study on a fleshy macroalgae in response to OA and provides new insights for this important functional group producing a large number of metabolites in response to their close environment.

## Graphical abstract

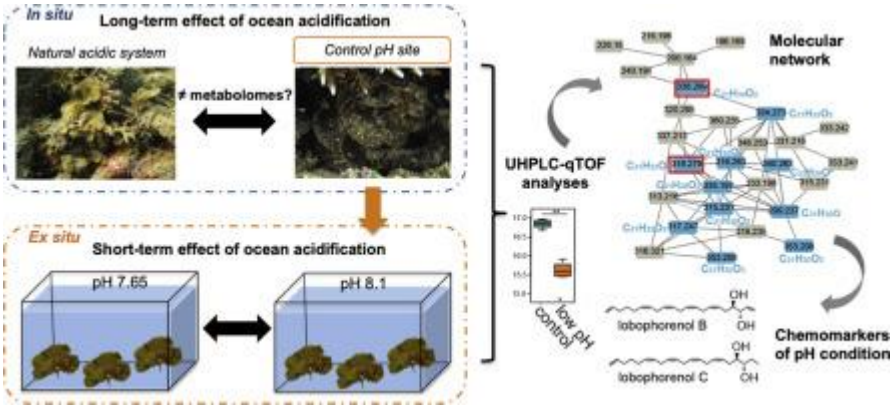


## Highlights

► Metabolomic responses of *Lobophora rosacea* are compared at different pH. ► Significant metabolomic differences are observed *in situ* between control and lower pH. ► An *ex situ* experiment demonstrates a short-term effect of ocean acidification. ► The concentration of metabolites related to lobophorenols decreases at low pH. ► We suggest a down-regulation of metabolic pathways involving oxylipins or their transformation when decreasing the pH

**Keywords** : Brown macroalgae, LC-MS, Metabolomics, Ocean acidification, Specialized metabolites

## Introduction

Rising emissions of atmospheric carbon dioxide ($CO_2$) due to human activities is leading to a phenomenon known as ocean acidification (OA), which is characterized by a decrease in seawater pH. Since the pre-industrial times, the average oceanic pH has already decreased by 0.1 unit, and it is expected to decrease by another 0.3-0.4 units by 2100 (Collins et al., 2013). Acceleration of OA is a global threat to a large range of organisms, impacting their physiological functions, life-history traits and behavior (e.g. Munday et al., 2014; Roggatz et al., 2016), and ultimately it will lead to population shifts (e.g. Doney et al., 2012; Gattuso et al., 2015).

Coral reefs, housing one of the largest diversity in the world and providing critical goods and services to coastal populations (Hughes et al., 2017; Moberg and Folke, 1999), are increasingly threatened by climate change (Cheal et al., 2017; Hughes et al., 2017). Predicting the responses of coral reefs to changing environmental conditions like OA is challenging because they support complex assemblages and interactions between organisms which may not all respond in the same way to such stressors (Ries et al., 2009) . For instance, heavily calcified organisms such as hard corals, bivalves and crustose coralline algae are expected to be highly sensitive to pH change, while organisms like fish or some crustaceans seem more able to compensate a decrease in extracellular pH (Kroeker et al., 2013, 2010). For non-calcifying macroalgae (i.e. fleshy macroalgae), the effect of OA has been shown to vary between species (e.g. (Diaz-Pulido et al., 2011; Gordillo et al., 2016; Xu et al., 2017), but their responses also depend on other factors such as developmental stages or carbon uptake mechanisms (e.g. passive $CO_2$ uptake without carbon-concentrating mechanism (CCM), or with CCM combined to high or low affinity for Dissolved Inorganic Carbon (DIC)) (Britton et al., 2016; Cornwall et al., 2017; Graba-Landry et al., 2018). Moreover, as observed in $C_3$-terrestrial plants, an increase in $CO_2$ would likely affect the production of allelochemicals in macroalgae (e.g. Bidart Bouzat and Adebobola, 2008; Swanson and Fox, 2007).

Macroalgae are critical components of coral reef ecosystems, providing shelter and food to countless species, and contributing to reef-building through cementation of the reef structure (e.g. coralline algae) (Egan et al., 2013; Webster et al., 2013). Their interaction with other species has been studied in some cases, especially when mediated by specialized metabolites deterrent of herbivores (e.g. Amsler, 2008; Cronin and Hay, 1996), but little is known of interactions with corals, with which they compete for space (Diaz-Pulido et al., 2011; Johnson et al., 2014; Rasher and Hay, 2010). Environmental or anthropogenic stresses or disturbances might favor macroalgae against corals and phase shifts from coral-dominated to macroalgae-dominated reefs are increasingly reported (Del Monaco et al., 2017; Holbrook et al., 2016). Such interactions often involve fleshy brown macroalgae species, like *Dictyota* spp. (Lirman and Biber, 2000), *Sargassum* spp. (Hughes, 1994; Ledlie et al., 2007) or

*Lobophora* spp. (Diaz-pulido et al., 2009), commonly encountered in tropical coral reef ecosystems, and mechanisms such as shading or abrasion, and chemical mediation (allelopathy) are usually mentioned (Del Monaco et al., 2017; McCook et al., 2001; Rasher and Hay, 2010). OA is likely to intensify such competitive interactions therefore accelerating ecological shifts towards reefs dominated by fleshy macroalgae, as already observed in $CO_2$ vents (Baggini et al., 2014; Fabricius et al., 2011; Hall-Spencer et al., 2008). However, the biochemical mechanisms involved in the response of fleshy macroalgae to OA are still poorly understood (Cornwall et al., 2017; Nunes et al., 2016) and previous studies have mainly focused on the effects of short to mid-term *ex situ* experiments that do not account for long-term acclimatisation and eventually adaptation to OA (e.g. Del Monaco et al., 2017; Duarte et al., 2016; Gordillo et al., 2016). Exceptions include observations and *in situ* experiments at $CO_2$ vents, as exemplified by Kumar et al. (2018) and Porzio et al. (2017) who highlight an increase of photochemical activity and a change in primary and secondary metabolites concentrations in *Sargassum vulgare* growing under natural acidic conditions near Ischia Island in Italy.

Environmental metabolomics is a growing technique used in marine science (Gaubert et al., 2019b; Greff et al., 2017a; Jaramillo et al., 2018; Viant, 2007) as it has a huge potential for exploring the responses of organisms to environmental conditions and for deciphering the metabolic pathways involved. Multi-stressor environments (e.g. physico-chemical variations, pathogen threats, anthropogenic stresses) induce acclimation of the physiological balance of organisms (e.g. for macroalgae Kumar et al., 2016), and one of the final phenotypic traits of cellular regulations is the biosynthesized metabolites, composing the broad metabolome (Fiehn, 2002; Kooke and Keurentjes, 2012). The recent development of analytical techniques in Liquid Chromatography-Mass Spectrometry (LC-MS) and Nuclear Magnetic Resonance (NMR) has allowed the observation and comparison of a global metabolome of more than thousands of metabolites in different experimental conditions. Metabolomic studies aiming at the exploration of the responses of marine organisms to OA were applied to different species including corals (Sogin et al., 2016), microbes (Coelho et al., 2015), crustaceans (Hammer et al., 2012) and bivalves (Ellis et al., 2014; Wei et al., 2015). However, to the best of our knowledge, no metabolomic study has been reported on the response of marine macroalgae to OA yet.

The aims of our study were: (a) to explore and compare metabolomic responses of brown macroalgae to both short- and long-term exposition to OA using *L. rosacea* as a model, and (b) to measure potential changes in macroalgal toxicity under OA. The recent discovery of a “natural analogue” of future climatic conditions at Bouraké (Camp et al., 2017), in New Caledonia, where seawater pH is similar to values predicted by the end of the century, provided an ideal natural environment to study long-term exposition of macroalgae to OA. The

brown fleshy macroalgal *Lobophora* (Dictyotaceae) was selected as it includes many species growing in various morphologies and habitats. This macroalgal genus is ecologically relevant in both shallow and deep reefs (Diaz-Pulido et al., 2011; Vieira et al., 2017, 2016, 2014) throughout the world and it is often observed in close association with corals in tropical ecosystems (notably in the Carribbean and in the Pacific (Jompa and Mccook, 2002; Mumby et al., 2005) and therefore involved in coral-algal interactions (Rasher and Hay, 2010), particularly with branching *Acropora* species (Vieira et al., 2016). In addition to *Lobophora* species thriving in close contact with scleractinian corals (e.g. *L. rosacea*, *L. hederacea* C.W. Vieira, Payri et De Clerck), some others are found abundantly in lagoons (e.g. *L. sonderii* C.W. Vieira, Payri et De Clerck) where, together with other brown macroalgae, they structure seaweed beds, essential habitats and nursery grounds for many small organisms (e.g. crustaceans, echinoderms, fish…) (Vieira, 2015). Among the 39 species of *Lobophora* recorded for New Caledonia (Vieira et al., 2014), we selected *Lobophora rosacea* C.W. Vieira, Payri et De Clerck, widespread across the lagoon and present at the natural analogue of Bouraké. Sampling strategies and experiments were designed to compare metabolomic fingerprints between populations present in Bouraké (long-term exposition to OA), in a control site (normal pH: no OA), and a controlled *ex situ* experiment (short-term exposition to both OA and control conditions).

## 2. Methods

### *2.1. Study sites and sampling for the in situ approach*

*Lobophora rosacea* was collected at two sites where it naturally grows in the southwest lagoon of New Caledonia*:* Bouraké (21°56.570'S; 165°59.310'E; July 2017) and Ricaudy (22°18.956'S; 166°27.405'E; August 2017; Fig. S1). The site we selected at Bouraké is a semi-enclosed system surrounded by mangroves where limited seawater circulation and biological activity contribute to increase the *p*CO2. The seawater pH fluctuates between 7.24 and 7.91 according to the tidal cycle (Camp et al., 2017), which we consider as representative of a natural analogue of future OA conditions. The populations of *L. rosacea* growing at this site are assumed to have been exposed to acidified levels over the long-term (probably even for several generations). Because no *L. rosacea* was found in the other prospected mangrove areas presenting a normal pH, the site of Ricaudy (well studied for this species (Gaubert et al., 2019b, 2019a) was selected as our control site. It is a fringing coral reef flat where the seawater $pH_T$ is 7.99 ± 0.03 ($pH_T$ = pH in total scale), which is considered as within the normal pH range for shallow coastal reef flats in New Caledonia. We assume that *L. rosacea* populations growing at this site

have never been exposed to abnormal pH conditions. While at Ricaudy, *Lobophora* was mostly found nested among branching corals (especially *Acropora* spp.; Fig. S2), in contrast at Bouraké, the species was particularly abundant on an area covered by coral rubble, where we collected the samples used during this study. Moreover, while other physical variables may slightly vary between Ricaudy and Bouraké, we only focused on the effect of pH, the most discriminant variable. For each site, eight samples (whole thalli) were randomly collected at 2-3 m deep by scuba diving, stored in separate plastic bags, and transported on ice in a cooler box before being frozen at -20 °C. Specimens of each sampling site were dried as herbarium vouchers and stored at the Institute of Research for Development (IRD) of Nouméa (see Fig. S3 for voucher numbers).

*2.2. Ex situ experiment*

For short-term experimental exposition to OA, a total of 53 samples of *L. rosacea* were carefully collected in August 2017, at the site of Ricaudy (control). Samples consisted of whole thalli (3 to 7 cm of diameter) randomly chosen, showing few visible epiphytes on their surface. They were kept alive in zip bags containing seawater from the sampling site and quickly transferred to the nearby *Aquarium des Lagons* (Nouméa, New Caledonia). Samples were randomly assigned to six 5 L seawater experimental tanks (n= 9 per tank). Light was provided by four T5 bulbs (6,000°K, Giesemann, Germany) supplying an irradiance of ca. 80-90 µmol photon $m^{-2}$ $s^{-1}$ over a 12 h dark/light cycle. Each tank received a continuous supply of filtered seawater (500 µm) pumped in the lagoon nearby the *Aquarium des Lagons* ($pH_T$ 8.13 ± 0.04) with an approximate flow rate of 130 mL $min^{-1}$. A submersible water pump (Mini-Jet, Aquarium Systems) gently mixed the seawater in each tank. Samples were acclimated during five days before pH was gradually decreased over a three-day period in three of the six tanks. The experimental $pH_T$ level was set to 7.65, which is in the range of the most pessimistic scenario for the end of century (scenario RCP 8.5; IPCC 2014) and comparable to the average pH measured at the natural analogue Bouraké. The three remaining tanks were considered as our control, and kept at pH of the seawater pumped nearby the *Aquarium des Lagons* ($pH_T$ 8.13 ± 0.04) which is representative of present-day conditions (Doney et al., 2012), and within the range of pH variation at the site of Ricaudy. In the experimental tanks, seawater pH was continuously controlled using a pH-stat system (Aquastar, IKS Computer System GmbH, Germany; precision ± 0.05 pH unit) that adjusts the pH by supplying pure $CO_2$ into the tanks. The computer control pH-stat system was verified twice a day for the duration of the experiment using a pH meter with a glass electrode (Metrohm 826 pH mobile) equipped with a Pt1000 temperature probe and an Aquatrode Plus pH electrode calibrated with Tris/HCl reference solutions (Dickson et al., 2007). After five days of acclimation and three days

of gradual pH decrease ($t_0$), three replicates per tank were sampled and frozen at -20°C. The six remaining samples were maintained under experimental conditions (acidification: $pH_T$ 7.65 ± 0.04, and control: $pH_T$ 8.13 ± 0.04; mean temperature: 23.9 ± 0.3 °C, Table S1) during another 14 days. At the end of the experiment ($t_{14}$), all samples were frozen at -20°C. The seawater carbonate chemistry was measured in each tank and is presented in supplementary Table S1.

*2.3. Metabolite extraction*

Samples collected from the natural analogue of Bouraké and the control site (16 samples hereafter referred to as "*in situ* samples") and during the *ex situ* experiment (53 samples, hereafter referred to as "*ex situ* samples") were freeze-dried and ground using liquid nitrogen. Metabolite extraction was done according to previous work on this alga (Gaubert et al., 2019b, 2019a). For each sample, 250 mg of the powder was extracted three times using 5 mL of MeOH/$CH_2Cl_2$ (1:1) during 5 min in an ultrasonic bath. After filtration of the supernatant (paper filter, 4-12 µm, Macherey-Nagel®), the crude extract was eluted on C18 silica powder (100 mg, Polygoprep 60-50, Macherey-Nagel®) by concentration under *vacuum* and fractionated on SPE cartridges (Strata C18-E 500 mg/6 mL, Phenomenex®) previously cleaned with 6 mL of MeOH/$CH_2Cl_2$ (1:1) and conditioned with 6 mL of milliQ $H_2O$. Each extract was fractioned by successive elution of $H_2O$, MeOH, and $CH_2Cl_2$ (6 mL of each solvent). MeOH fractions were filtered on syringe filters (PTFE, 0.20 µm, Phenomenex®) and further analyzed by Ultra High Pressure Liquid Chromatography coupled to Quadrupole-Time of Flight mass spectrometer (UHPLC-QqToF). Due to the high concentration in salt, which inhibits MS-based metabolomics analysis, $H_2O$ fractions were not analyzed. $CH_2Cl_2$ fractions are more suitable for GC-MS analyses and were not analyzed in this study. The algal metabolome referred then to the MeOH extracts through the text, which contain a majority of secondary metabolites, including allelopathic compounds (e.g. (Gaubert et al., 2019a)).

*2.4. Metabolomic analyses*

Metabolomic analyses were performed using a UHPLC (Dionex Ultimate 3000, Thermo Scientific®) coupled to a mass spectrometer (MS)QqToF equipped with an electrospray ion source (Impact II, Bruker Daltonics®). Chromatographic separation of metabolites was performed on an Acclaim™ RSLC 120 C18 column (2.1 x 150 mm, 2.2 µm, Thermo Scientific®) at a constant temperature of 40 °C. The mobile phase was prepared with $H_2O$ + 0.1% formic acid + 10 mM ammonium formate (A), and acetonitrile/$H_2O$ (95/5) + 0.1% formic acid + 10 mM

ammonium formate (B). The optimized elution gradient was programed as follows: 60% A – 40% B during 2 min, a linear gradient up to 100% B from 2 to 8 min, an isocratic step of 100% B during 4 min, and return to the initial conditions from 12 to 14 min. A post-run step of 3 min was set for column equilibration (60% A – 40% B) after analysis for a total runtime of 17 min. Injection volume was set to 5 µL and the elution rate to 0.5 mL $min^{-1}$. Mass spectra were acquired in positive mode. Negative ionization mode was tested in our preliminary work on *L. rosacea* (Gaubert, 2018) but resulted in fewer detected compounds compared to positive mode and was not retained. MS parameters were set as follows: nebulizer gas $N_2$ at 40 psi, gas temperature: 200 °C, drying gas $N_2$ at 4 L $min^{-1}$, spectra acquisition at 2 Hz from *m/z* 50 to 1200, capillary voltage: 3500 V. Auto-$MS^2$ were acquired in the same conditions. A quality control sample (QC) was prepared with 25 µL of each sample. The run started with three blank injections, followed by 10 injections of the QC sample for spectrometer stabilization. The samples were then injected randomly, including a QC sample every five samples, allowing an assessment of MS shift over time and data normalization. A final blank was injected to check any memory effect of the compounds on the column.

LC–MS raw data files were calibrated before converting them to netCDF files (centroid mode) using Bruker Compass DataAnalysis 4.3. NetCDF files were processed using the package XCMS (Smith et al., 2006) for R software (R version 3.3.2, XCMS version 1.50.1). Optimized parameters for XCMS script were used as follows: peak detection (method= “centwave”, peakwidth= c(2,20), ppm= 15, mzdiff= 0.05, prefilter= c(0,0)), retention time correction (method= “obiwarp”, plottype= “deviation”), matching peaks across samples (bw= 30, mzwid= 0.015, minfrac= 0.3, minsamp=1), and filling in missing peak data. To remove technical variability, the matrix was then filtered according to blanks and QC using in-house R scripts: 1- filtering the matrix according to peaks present in blanks relative to QC (signal/noise ratio > 10), 2- filtering the matrix according to peaks coefficient of variation (CV) calculated on QC (CV > 20%), and 3- filtering the matrix according to autocorrelation between peaks. The final matrix was composed of ions with an integrated peak area for each *m/z* value and retention time. Data were log-transformed prior to statistical analysis. A molecular networks based on $MS^2$ spectra was constructed with GNPS (Wang et al., 2016) using the following settings : precursor ion mass tolerance: 2 Da, fragment ion mass tolerance: 0.5 Da, min pairs cos: 0.7, minimum matched fragment ion: 6, node topK: 10 and minimum cluster size: 2 . Resulting networks were observed under Cytoscape 3.5.0 (Shannon et al., 2003). Metlin (https://metlin.scripps.edu/ (Smith et al., 2005)), in-house library and SIRIUS 4.0. (Böcker and Dührkop, 2016) were also used for putative annotation.

*2.5 Bioactivity test*

The standardized Microtox® assay was used (Johnson 2005, R-Biopharm®, France) as a rapid proxy of sample toxicity against marine micro-organisms. Bioactivity was measured as the effect of extracts on the metabolism of the bioluminescent marine bacteria *Aliivibrio fischeri*. Stock solutions of MeOH fractions were prepared at 2 mg $mL^{-1}$ in artificial seawater with 2% acetone to facilitate dissolution. Stock solutions were then diluted at 0.4 mg $mL^{-1}$, and diluted again three times by a factor two to draw $EC_{50}$ curves. Measures of bacterial bioluminescence were recorded after 5 min of exposure to fractions. For relevant ecological comparison, γ units relative to 1 mg of sample per mL of solution were calculated as described in (Greff et al., 2014). Bioactivities (or toxicities) of MeOH extracts were not assessed for samples collected during the *ex situ* experiment.

*2.6 Statistical analyses*

Statistical analyses were performed using the R software. The normality of the data distribution was tested using the Shapiro-Wilk test and the homogeneity of variances with the Levene test. Because the homogeneity of variance was confirmed but not the normality, the Student's test with permutations (RVAideMemoire package) was used to test the pH difference between tank treatments. A principal component analysis (PCA) was constructed to visualize the metabolome variation as a function of pH conditions (R ade4 package). A Powered Partial Least-Squares-Discriminant Analysis (PPLS-DA) allowed finding the maximum covariance between our dataset, and their class membership, while the permutational tests based on cross-model validation (MVA.test and pairwise.MVA.test) were used to test differences between groups (i.e. low *vs* control pH; RVAideMemoire package, CER= Classification Error Rate). Discriminating compounds (chemomarkers or VIP: Variable Importance in Projection) were identified according to the PPLS-DA loading plots (correlation circles using a threshold of 0.8; RVAideMemoire package). The Wilcoxon's test was used to check differences in $EC_{50}$ and chemomarker intensities between control and low pH sites (mean ± SD). Finally, the Kruskal-Wallis' test was used to identify differences in normalized intensities of chemomarkers between pH treatments for the *ex situ* experiments. Venn diagrams were constructed using the Vennerable package.

## 3. Results

### *3.1. Long-term exposition to OA*

After LC-MS data treatment and filtering, the matrix resulted in 262 features that were used for the construction of the PCA (Fig. S4). The first two components explained 48.02% of the variance, and two significantly distinct clusters (Bouraké *vs* Ricaudy) were identified using a PPLS-DA (CER = 0, p = 0.001, Fig. 1a). According to the Venn diagram (Fig. S5), the differences between the metabolomic fingerprints of samples from the low pH and the control sites were only quantitative. A total of 53 metabolites (chemomarkers) were driving these differences (threshold of 0.8, Fig. 1b). Their putative molecular formula (Table S2) was deduced from accurate mass measurement, isotopic and fragmentation patterns, and our previous chemical work on *L. rosacea*. Compared to control pH conditions, about 30% (16) of the chemomarkers were over-represented in low pH conditions, while 70% (37) were under-represented Among them, we identified some putative polyunsaturated compounds with 21 carbons and one to three oxygen atoms, including the polyunsaturated alcohols lobophorenols B and C previously isolated in *L. rosacea* (Vieira et al., 2016), which are standards present in our library, and some C20-C24 oxygenated fatty acid analogues, all under-represented in low pH condition. Metabolites with higher molecular weights (C26-C35 and up to 7 oxygen atoms) and several minor intensity ions also participated in the discrimination between low pH and control conditions.

### *3.2. Bioactivity assays*

Bioactivity assays on MeOH extracts using Microtox® showed that these extracts are bioactive according to Martí et al. (2004) who set the threshold between non-toxic and toxic samples at 0.5 γ units. However, no significant difference in toxicity between the two sites was recorded ($\gamma = 0.67 \pm 0.08$ and $0.55 \pm 0.16$, from control and low pH sites, respectively; n = 8, Wilcoxon rank sum test, p = 0.13, Fig. S6).

### *3.3. Short-term exposition to OA*

Metabolomic responses were measured at the start of the experiment ($t_0$, i.e. after the acclimation period and gradual decrease of pH to reach $pH_T$ 7.65 in the experimental tanks), and after 14 days ($t_{14}$) of low ($pH_T$ 7.65) or control ($pH_T$ 8.1) pH treatments. Using PPLS-DA analyses, we found significant differences between the metabolomes of the MeOH extracts in the control and low pH samples at both $t_0$ and $t_{14}$ ($CER_{t0} = 0.05$; $CER_{t14} = 0.07$, p = 0.001; Fig. 2a). Except for one specific compound found at $t_0$ in the low pH treatment samples (M722T301), only quantitative changes in metabolites were recorded (Venn diagram, Fig. S7). The

chemomarkers driving metabotype differences between the two pH treatments were selected according to PPLS-DA loading plots (Fig. 2b, threshold 0.8), and tentatively annotated in Table S3 based on accurate mass measurement, isotopic and fragmentation patterns. Twelve of them were determined at $t_0$, among which five were over-represented and seven under-represented in low pH compared to control conditions (C21-C29 and up to 6 oxygen atoms), including lobophorenol C. At $t_{14}$, 10 markers were over-represented in low pH treatments and none were under-represented compared to the control. Three of these compounds were putatively annotated as polyunsaturated oxygenated fatty acid derivatives with 16 to 20 carbon and three oxygen atoms.

### *3.4. Chemomarkers of pH conditions: in situ samples and ex situ experiment*

Among the metabolites, a total of 53 chemomarkers were identified in samples collected from the low pH (Bouraké) and the control (Ricaudy) sites (i.e. *in situ* samples). A second set of 22 chemomarkers was identified during the *ex situ* experiment. Molecular formulae were established based on the comparison of their masses and isotopic patterns with theoretical ones (Tables 1, S2 and S3). A molecular network was also constructed from $MS^2$ spectra of the complete metabolomic dataset and used to determine similarities between compounds to help in chemomarker annotation. We also used the SIRIUS software to strengthen their annotation. One cluster of the network (Fig. 3) included 10 out of the 75 previously highlighted chemomarkers (in Figures 1b and 2b). It included lobophorenols B (*m/z* 334.2742 $[M + NH_4]^+$, $C_{21}H_{32}O_2$; M334T515) and C (*m/z* 336.2896 $[M + NH_4]^+$, $C_{21}H_{34}O_2$; M336T524), and seven analogues of lobophorenol B. Except for one analogue with 23 carbons, they all contain 21 carbons, with one to three oxygen atoms, and six to eight unsaturations (Table 1a). These 10 markers were under-represented in all low pH samples (i.e. from the site of Bouraké or the tank experiment; see Fig. 4).

A Venn diagram was also produced to highlight possible similarities between the different sets of chemomarkers of pH conditions (Fig. 5). It revealed that, out of the 53 and 22 markers identified from the *in situ* and *ex situ* samples respectively, 10 were common. Six of these metabolites were shared between *in situ* and *ex situ* $t_0$ samples (M318T600, M336T524, M345T499, M363T470, M438T479, M459T477), and they were present in lower quantities in low pH samples than in control samples (both *in situ* and *ex situ*). Four chemomarkers were shared between *in situ* and *ex situ* $t_{14}$ samples (M344T543, M555T641, M598T638, M644T635), and present in larger quantities in low pH samples (Fig. 5, Table 1b). No chemomarker was shared between *ex situ* $t_0$ and $t_{14}$

samples. In total, 65 unique chemomarkers of pH conditions (low or control) were recorded in both sets of samples.

Among the chemomarkers present in both *in situ* and *ex situ* $t_0$ samples, several unsaturated oxygenated fatty acids that likely contain 20 to 29 carbons and three to six oxygen atoms were annotated (Table 1b). We also found lobophorenol C ($C_{21}H_{34}O_2$), and the unidentified compound $C_{21}H_{32}O$, which are both present in the cluster (Fig. 3, Table 1a). The compound $C_{21}H_{32}O$ could correspond to an epoxide or unsaturated ketone. Among the chemomarkers shared by *in situ* and *ex situ* $t_{14}$ samples, we putatively annotated an unsaturated compound with 20 carbons and three oxygen atoms, while the others remained unknown (Table 1b).

## 4. Discussion

We investigated metabolomic changes in the methanol extracts induced by both short- and long-term exposition to OA in the common fleshy tropical macroalgae *L. rosacea.* Our results revealed significant metabolomic differences between *L. rosacea* samples exposed to low pH during their whole life cycle (possibly for several generations; site of Bouraké), compared to samples from a control site (Ricaudy Reef). Differences were also found during short-term *ex situ* experiment, at the beginning (t0) and at the end (t14). Some different metabolites were involved, which could be due to the very rapid acclimation time (3 days) in tank experiment compared to the natural analogue (several generations).

The metabolic differences observed between the control and low pH samples were mostly quantitative (cf. Venn diagrams, Fig. 5), suggesting metabolic plasticity in response to low pH levels. Our results demonstrate that *L. rosacea* can adapt some metabolic pathways in response to low pH conditions over both the short- and long-terms. In doing so, it regulates the production of selected specialized metabolites over time. Our analyses isolated a total of 65 unique chemomarkers of pH conditions, among which 59% were under-represented and 41% over-represented in low pH compared to control conditions regarding both experiments (short and long-term exposition to OA). Ten of the 65 chemomarkers were common to both *in situ* and *ex situ* samples. Among the chemomarkers under-represented at low pH, two of them recently described as lobophorenols B and C, are specialized polyunsaturated oxylipins previously isolated from *L. rosacea* by Vieira et al. (2016). Other related polyunsaturated metabolites were also identified. The latter are likely close derivatives of lobophorenols, as they

contain 21 carbons and one to three oxygen atoms. Using *in situ* bioassays in the lagoon of New Caledonia, Vieira et al. (2016) demonstrated that lobophorenols induce allelopathic activity against the coral *Acropora muricata* (bleaching) and no other biological function of these metabolites is recorded in the literature. Similar C21 apolar compounds, with terminal vinylic protons but no oxygen atom, have been reported in *Fucus vesiculosus* (Halsall and Hills, 1971) and could possibly have a protective role against pathogens or herbivores (Youngblood and Blumer, 1973). At low pH, some putative C16-C20 polyunsaturated oxygenated fatty acid derivatives were over-represented, while putative C20-C24 compounds were under-represented compared to control conditions. As lobophorenols and other C21 analogues should derive from the corresponding C22 polyunsaturated fatty acids following a decarboxylative process, we hypothesize that the conversion of C22 derivatives into lobophorenols is somehow inhibited in a low pH environment. Reversely, lobophorenols can also be catabolized into shorter metabolites at low pH but the first hypothesis seems more likely. The significant decrease in lobophorenol related metabolites at low pH would therefore be in agreement with the optimal defense theory (Cronin, 2001; Ivanišević et al., 2011), where primary biological functions, like homeostasis, growth or reproduction are maintained in a stressful environment, while less energy is dedicated to the production of specialized metabolites (Cronin, 2001; López-Legentil et al., 2006). Further physiological measures (like growth) would be necessary to support this hypothesis. It is also possible that lobophorenols and C21 analogues were released in the surrounding environment, another hypothesis which could be explored by analysis of the exometabolome. Indeed, an increase in dissolved organic carbon under high CO2 conditions has been observed in some macro- and micro-algae (Giordano et al., 1994; Iñiguez et al., 2016), a phenomenon that could also occur in our experimental conditions.

Other chemomarkers linked to pH conditions were isolated in our study but we could not identify their structures using databases like GNPS or Metlin but also some in silico fragmentation like SIRIUS. For marine organisms, and especially non-model organisms, metabolite annotation is often limited by a lack of standards (*e.g.* Gaubert et al., 2019b, 2019a, Greff et al., 2017b, 2017a; Sogin et al., 2016). This issue is one of the greatest challenges in untargeted metabolomic studies (Kumar et al., 2016). Because we only analyzed the methanol fraction of our samples, the chemomarkers identified in our study represent only a part of the metabolic changes occurring in *L. rosacea* when exposed to low pH as chemical variations may also occur in the polar (water fraction) and apolar fractions (dichloromethane) likely to contain more primary metabolites.

Even though responses to elevated $CO_2$ concentrations (i.e. to a pH decrease) seem to be species-specific (Arnold et al., 2012; Swanson and Fox, 2007), changes in specialized phenolic compounds, which are involved

in several functions (e.g. deterrence, antimicrobial, UV protector or cell wall structure (Gutow et al., 2014)), have been observed in most marine plants and macroalgae (e.g. Betancor et al., 2014; Del Monaco et al., 2017; Kumar et al., 2018). Some *Lobophora* species are known to produce phenolic compounds (e.g. *L. variegatea;* Chkhikvishvili and Ramazanov, 2000), but our previous extensive chemical work on *L. rosacea* did not reveal any phenolics (Gaubert, 2018; Vieira, 2015), which are likely minor compounds in this species. A decrease in specialized metabolites in macroalgae under OA can also have consequences on their commercial uses. Although *Lobophora* is not currently marketed, macroalgae are an important source of specialized metabolites, particularly polyphenols, used for different applications including pharmaceutical, nutraceutical, cosmeceutical or antifouling industries (e.g. Calado et al., 2018).

As algal specialized metabolites can also be involved in the chemical mediation with other organisms, and notably in allelopathic interactions with corals, its crucial to understand how OA may affect these metabolites and their bioactivity. This is even more pertinent as phase shifts from coral-dominated to macroalgae-dominated reefs are increasingly reported (Del Monaco et al., 2017; Holbrook et al., 2016). *Lobophora* is particularly significant in this context. According to Koch et al. (2013), *Lobophora* species have a C3 photosynthetic pathway for carbon fixation, and their capacity to fix $CO_2$ increases linearly with the quantity of available $CO_2$, until the Rubisco enzyme becomes saturated (Holbrook et al., 1988; Koch et al., 2013; Yamori et al., 2014). It was highlighted that, as seen in terrestrial C3 communities, a $CO_2$ concentration increase may benefit C3 non-calcareous algae (Diaz-Pulido et al., 2011; Koch et al., 2013), and is also likely to induce a modification in the C:N ratio, possibly altering the macroalgae nutritional quality for herbivores and their palatability (Alstyne et al., 2009; Arnold et al., 1995; Gutow et al., 2014; Kumar et al., 2018; Swanson and Fox, 2007). This suggests that species of fleshy macroalgae, like *Lobophora*, could thrive in high *p*CO2 conditions while it would be detrimental to corals and other calcifying species (Anthony et al., 2008; Diaz-Pulido et al., 2011; Ragazzola et al., 2012). In addition, over the last four decades, increased abundances of *Lobophora* have been observed on many degraded reefs, especially in the Caribbean and Indo-Pacific, rising concerns on its potential deleterious effects on corals (Del Monaco et al., 2017; Fricke et al., 2011; Nugues and Bak, 2008; Slattery and Lesser, 2014). During an eight-week experiment, Diaz-Pulido et al. (2011) demonstrated that OA enhances the ability of *Lobophora papenfusii* W.R. Taylor to affect and potentially overgrow the coral *Acropora intermedia* possibly *via* either chemical or biological effect. Vieira et al. (2016) also demonstrated that the pure lobophorenols B and C of *L. rosacea* can be allelopathic against the corals *Acropora muricata*. Our rapid bioassays, targeted on the

bacteria *Vibrio fischerii*, confirmed the toxicity of *L. rosacea* MeOH extracts, containing lobophorenols as well as other metabolites, but there was no significant difference in bioactivity between samples collected from the natural analogue of Bouraké (low pH) and the control site. These results suggest that the lower concentration in lobophorenols of the extracts from the low pH samples was compensated by other bioactive compounds. For instance, lipidic and hydrophobic compounds can be involved in the chemical mediation with other organisms, notably with corals (Andras et al., 2012; Del Monaco et al., 2017; Rasher and Hay, 2014). Our results, however, must be interpreted with caution, as we only tested the bioactivity of the extracts on a proxy marine bacterium (Microtox® bioassays), which is likely to respond differently compared to more complex organisms like corals. Further investigation is needed, including coral-algal interaction experiments (e.g. Del Monaco et al., 2017; Greff et al., 2017a), to evaluate the potential impact of *L. rosacea* on corals in the context of ocean acidification. The natural analogue of Bouraké, where sessile organisms have been acclimated for several generations, could represent a relevant system for this investigation.

**Conclusion**

Our study is the first to explore the effects of ocean acidification on the metabolome of fleshy marine macroalgae via an untargeted metabolomics approach. Using a novel natural analogue of future oceanic pH conditions, the lagoon of Bouraké in New Caledonia, and an *ex situ* experiment, we found significant metabolomic changes in *L. rosacea* exposed to low pH, and different metabolomic fingerprints between long-term (several generations) and short-term (two weeks) expositions. Our main finding is a decrease in some specialized metabolites at low pH compared to control conditions, which we relate to the optimal defense theory, but similar bioactivity. Among the 65 chemomarkers of pH targeted, two allelopathic compounds were unambiguously annotated, lobophorenols B and C, and several related C21 oxygenated polyunsaturated fatty acids derivatives, which were all under-represented at low pH. With the assumption that lobophorenols play a role in coral-algal competition, OA-like conditions did not appear to favor the allelopathy of the fleshy macroalgae. This is in accordance with our observations at the site we explored in the natural analogue of Bouraké, where no *Lobophora* was found growing on corals, the latter being unexpectedly well developed for a low pH environment, with tens of species of corals inhabiting this site.

Additional studies will need to overcome the limitations of metabolite characterization, explore highly polar/non-polar fractions, and carry out *in situ* bioassays to confirm the level of toxicity of *Lobophora* in acidified conditions. Lipid-profiling would also be an interesting approach to further explore and understand the

metabolic pathways involved in the responses of *L. rosacea* to OA. Sea Surface Temperature is another critical variable of climate change, which is likely to act in combination with OA and should be taken into account in future studies. Natural analogues of future climatic conditions, such as the lagoon of Bouraké in New Caledonia, provide ideal natural laboratories to study the effects of OA over the long-term, on both individual species and their interactions. The study of the metabolome is an interesting approach for further work on the effects of climate change on macroalgae, particularly because metabolites are involved in many functions like deterrence or homeostasis. Metabolomic fingerprint can provide a wide picture to understand the different biochemical pathways involved and re-programmed under environmental perturbations. Chemistry is highly linked to biology and can provide important information to better understand and predict how marine organisms, not only macroalgae, will adapt or evolve in our future ocean.

**Acknowledgments**: The PhD project of J. Gaubert was supported by a scholarship of Sorbonne University, Paris, France. This project was partially supported by ANR PNG-Vents: ANR-17-ERC2-0009. Part of this project was carried out with the support of the Marine Institute (Grant-Aid Agreement No. PBA/MB/16/01) and is funded under the Marine Research Program by the Irish Government. We are grateful to J-C. Martin for the R scripts that he has designed for the matrix filtration and to M. Zubia (University of French Polynesia) for her useful comments. Thanks to the Aquarium des lagons (Nouméa, New Caledonia) for hosting the tanks during the *ex-situ* experiment. We thank T. Pérez for hosting J. Gaubert at the Station Marine d'Endoume (Marseille, France) where metabolomic analyses were performed on the Mallabar Regional platform (funded by the CNRS and the Provence Alpes Côte d'Azur Region).

**Competing Interests:** The authors declare no competing interests.

**Author Contributions:** J.G., R.R.M., O.T. and C.P. designed the experiments. J.G. performed algal collections under the supervision of C.P. and R.R.M. J.G. and R.R.M set up the aquaria experiment. J.G. carried out extractions and fractionations. J.G. and S.G. analyzed metabolomic fingerprints and bioactivity. J.G. performed data analyses. J.G. drafted the manuscript with input from all authors. J.G. reviewed the manuscript.

**Data availability**: Metabolomics data have been deposited to the EMBL-EBI MetaboLights database (DOI:

10.1093/nar/gks1004. PubMed PMID: 23109552) with the identifier MTBLS1038.

The complete dataset can be accessed here https://www.ebi.ac.uk/metabolights/MTBLS1038

## References


Alstyne, K.L. Van, Pelletreau, K.N., Kirby, A., 2009. Journal of Experimental Marine Biology and Ecology Nutritional preferences override chemical defenses in determining food choice by a generalist herbivore , Littorina sitkana. J. Exp. Mar. Bio. Ecol. 379, 85–91. https://doi.org/10.1016/j.jembe.2009.08.002

Amsler, C.D., 2008. Algal chemical ecology, Algal Chemical Ecology. https://doi.org/10.1007/978-3-540-74181-7

Andras, T.D., Alexander, T.S., Gahlena, A., Parry, R.M., Fernandez, F.M., Kubanek, J., Wang, M.D., Hay, M.E., 2012. Seaweed Allelopathy Against Coral: Surface Distribution of a Seaweed Secondary Metabolite by Imaging Mass Spectrometry. J. Chem. Ecol. 38, 1203–1214. https://doi.org/10.1007/s10886-012-0204-9

Anthony, K.R.N., Kline, D.I., Diaz-Pulido, G., Dove, S., Hoegh-Guldberg, O., 2008. Ocean acidification causes bleaching and productivity loss in coral reef builders. Proc. Natl. Acad. Sci. 105, 17442–17446. https://doi.org/10.1073/pnas.0804478105

Arnold, T., Mealey, C., Leahey, H., Miller, A.W., Hall-spencer, J.M., Milazzo, M., Maers, K., 2012. Ocean Acidification and the Loss of Phenolic Substances in Marine Plants 7, 1–10. https://doi.org/10.1371/journal.pone.0035107

Arnold, T.M., Tanner, C.E., Hatch, W.I., 1995. Phenotypic variation in polyphenolic content of the tropical brown alga Lobophora variegata as a function of nitrogen availability. Mar. Ecol. Prog. Ser. 123, 177–184. https://doi.org/10.3354/meps123177

Baggini, C., Salomidi, M., Voutsinas, E., Bray, L., Krasakopoulou, E., Hall-Spencer, J.M., 2014. Seasonality affects macroalgal community response to increases in pCO2. PLoS One 9, 1–13. https://doi.org/10.1371/journal.pone.0106520

Betancor, S., Tuya, F., Gil-Díaz, T., Figueroa, F.L., Haroun, R., 2014. Effects of a submarine eruption on the performance of two brown seaweeds. J. Sea Res. 87, 68–78. https://doi.org/10.1016/j.seares.2013.09.008

Bidart Bouzat, M., Adebobola, I.N., 2008. Global change effects on plant chemical defenses against insect herbivores. J. Integr. Plant 50, 1339–1354. https://doi.org/10.1111/j.1744-7909.2008.00751.x

Böcker, S., Dührkop, K., 2016. Fragmentation trees reloaded. J. Cheminform. 1–26. https://doi.org/10.1186/s13321-016-0116-8

Britton, D., Cornwall, C.E., Revill, A.T., Hurd, C.L., Johnson, C.R., 2016. Ocean acidification reverses the positive effects of seawater pH fluctuations on growth and photosynthesis of the habitat-forming kelp, Ecklonia radiata. Sci. Rep. 6, 1–10. https://doi.org/10.1038/srep26036

Camp, E.F., Nitschke, M.R., Rodolfo-metalpa, R., Houlbreque, F., Gardner, S.G., Smith, D.J., Zampighi, M., Suggett, D.J., 2017. Reef-building corals thrive within hot-acidified and deoxygenated waters. Sci. Rep. 7, 1–9. https://doi.org/10.1038/s41598-017-02383-y

Cheal, A.J., MacNeil, M.A., Emslie, M.J., Sweatman, H., 2017. The threat to coral reefs from more intense cyclones under climate change. Glob. Chang. Biol. 23, 1511–1524. https://doi.org/10.1111/gcb.13593

Chkhikvishvili, I.D., Ramazanov, Z.M., 2000. Phenolic substances of brown algae and their antioxidant activity. Appl. Biochem. Microbiol. 36, 289–291. https://doi.org/10.1007/BF02742582

Coelho, F.J.R.C., Cleary, D.F.R., Rocha, R.J.M., Calado, R., Castanheira, J.M., Rocha, S.M., Silva, A.M.S., Simões, M.M.Q., Oliveira, V., Lillebø, A.I., Almeida, A., Cunha, Â., Lopes, I., Ribeiro, R., Moreira-Santos, M., Marques, C.R., Costa, R., Pereira, R., Gomes, N.C.M., 2015. Unraveling the interactive effects

of climate change and oil contamination on laboratory-simulated estuarine benthic communities. Glob. Chang. Biol. 21, 1871–1886. https://doi.org/10.1111/gcb.12801

Collins, M., Knutti, R., Arblaster, J., Dufresne, J.-L., Fichefet, T., Friedlingstein, P., Gao, X., Gutowski, W.J., Johns, T., Krinner, G., Shongwe, M., Tebaldi, C., Weaver, A.J., Wehner, M., 2013. Long-term Climate Change: Projections, Commitments and Irreversibility, in: Climate Change 2013: The Physical Science Basis. Contribution of Working Group I to the Fifth Assessment Report of the Intergovernmental Panel on Climate Change. pp. 1029–1136. https://doi.org/10.1017/CBO9781107415324.024

Cornwall, C.E., Revill, A.T., Hall-Spencer, J.M., Milazzo, M., Raven, J.A., Hurd, C.L., 2017. Inorganic carbon physiology underpins macroalgal responses to elevated CO2. Sci. Rep. 7, 1–12. https://doi.org/10.1038/srep46297

Cronin, G., 2001. Ressource allocation in Seaweeds and Marine Invertebrates: Chemical Defense Patterns in Relation to Defenses Theories. Mar. Chem. Ecol. https://doi.org/10.1201/9781420036602.ch9

Cronin, G., Hay, M.E., 1996. Induction of Seaweed Chemical Defenses by Amphipod Grazing. Ecology 77, 2287–2301.

Del Monaco, C., Hay, M.E., Gartrell, P., Mumby, P.J., Diaz-Pulido, G., 2017. Effects of ocean acidification on the potency of macroalgal allelopathy to a common coral. Sci. Rep. 7, 1–10. https://doi.org/10.1038/srep41053

Diaz-Pulido, G., Gouezo, M., Tilbrook, B., Dove, S., Anthony, K.R.N., 2011. High CO2 enhances the competitive strength of seaweeds over corals. Ecol. Lett. 14, 156–162. https://doi.org/10.1111/j.1461-0248.2010.01565.x

Diaz-pulido, G., Mccook, L.J., Dove, S., Berkelmans, R., Roff, G., David, I., Weeks, S., Evans, R.D., Williamson, D.H., Hoegh-guldberg, O., 2009. Doom and Boom on a Resilient Reef : Climate Change , Algal Overgrowth and Coral Recovery. PLoS One 4. https://doi.org/10.1371/journal.pone.0005239

Dickson, A.G., Sabine, C.L., R, C.J., 2007. Guide to best practices for ocean CO2 measurements., PICES Special Publication. https://doi.org/10.1159/000331784

Doney, S.C., Ruckelshaus, M., Emmett Duffy, J., Barry, J.P., Chan, F., English, C.A., Galindo, H.M., Grebmeier, J.M., Hollowed, A.B., Knowlton, N., Polovina, J., Rabalais, N.N., Sydeman, W.J., Talley, L.D., 2012. Climate Change Impacts on Marine Ecosystems. Ann. Rev. Mar. Sci. 4, 11–37. https://doi.org/10.1146/annurev-marine-041911-111611

Duarte, C., López, J., Benítez, S., Manríquez, P.H., Navarro, J.M., Bonta, C.C., Torres, R., Quijón, P., 2016. Ocean acidification induces changes in algal palatability and herbivore feeding behavior and performance. Oecologia 180, 453–462. https://doi.org/10.1007/s00442-015-3459-3

Egan, S., Harder, T., Burke, C., Steinberg, P., Kjelleberg, S., Thomas, T., 2013. The seaweed holobiont: Understanding seaweed-bacteria interactions. FEMS Microbiol. Rev. 37, 462–476. https://doi.org/10.1111/1574-6976.12011

Ellis, R.P., Spicer, J.I., Byrne, J.J., Sommer, U., Viant, M.R., White, D.A., Widdicombe, S., 2014. 1H NMR metabolomics reveals contrasting response by male and female mussels exposed to reduced seawater pH, increased temperature, and a pathogen. Environ. Sci. Technol. 48, 7044–7052. https://doi.org/10.1021/es501601w

Fabricius, K.E., Langdon, C., Uthicke, S., Humphrey, C., Noonan, S., De, G., Okazaki, R., Muehllehner, N., Glas, M.S., Lough, J.M., 2011. Losers and winners in coral reefs acclimatized to elevated carbon dioxide concentrations. Nat. Clim. Chang. 1, 165–169. https://doi.org/10.1038/nclimate1122

Fiehn, O., 2002. Metabolomics - the link between genotyopes and phenotypes. Plant Mol. Biol. 48, 155–171. https://doi.org/https://doi.org/10.1023/A:1013713905833

Fricke, A., Titlyanova, T. V, Nugues, M.M., Bischof, K., 2011. Depth-related variation in epiphytic communities growing on the brown alga Lobophora variegata in a Caribbean coral reef. Coral Reefs 30, 967–973. https://doi.org/10.1007/s00338-011-0772-0

Gattuso, J.P., Magnan, A., Billé, R., Cheung, W.W.L., Howes, E.L., Joos, F., Allemand, D., Bopp, L., Cooley, S.R., Eakin, C.M., Hoegh-Guldberg, O., Kelly, R.P., Pörtner, H.O., Rogers, A.D., Baxter, J.M., Laffoley,

D., Osborn, D., Rankovic, A., Rochette, J., Sumaila, U.R., Treyer, S., Turley, C., 2015. Contrasting futures for ocean and society from different anthropogenic CO2emissions scenarios. Science (80-. ). 349. https://doi.org/10.1126/science.aac4722

Gaubert, J., 2018. Caractérisation et sources de variation du métabolome : le cas de l'algue brune *Lobophora* des écosystèmes coralliens de Nouvelle-Calédonie.

Gaubert, J., Greff, S., Thomas, O.P., Payri, C.E., 2019a. Metabolomic variability of four macroalgal species of the genus Lobophora using diverse approaches. Phytochemistry 162, 165–172. https://doi.org/10.1016/j.phytochem.2019.03.002

Gaubert, J., Payri, C.E., Vieira, C., Solanki, H., Thomas, O.P., 2019b. High metabolic variation for seaweeds in response to environmental changes : a case study of the brown algae Lobophora in coral reefs. Sci. Rep. 1–12. https://doi.org/10.1038/s41598-018-38177-z

Giordano, M., Davis, J.S., Bowes, G., 1994. Organic carbon release by Dunaliella salina (Chlorophyta) under different growth conditions of CI2, nitrogen and salinity. J. Phycol. 30, 249–257.

Gordillo, F.J.L., Carmona, R., Viñegla, B., Wiencke, C., Jiménez, C., 2016. Effects of simultaneous increase in temperature and ocean acidification on biochemical composition and photosynthetic performance of common macroalgae from Kongsfjorden (Svalbard). Polar Biol. 39, 1993–2007. https://doi.org/10.1007/s00300-016-1897-y

Graba-Landry, A., Hoey, A.S., Matley, J.K., Sheppard-Brennand, H., Poore, A.G.B., Byrne, M., Dworjanyn, S.A., 2018. Ocean warming has greater and more consistent negative effects than ocean acidification on the growth and health of subtropical macroalgae. Mar. Ecol. Prog. Ser. 595, 55–69. https://doi.org/10.3354/meps12552

Greff, S., Aires, T., Serrão, E.A., Engelen, A.H., Thomas, O.P., Pérez, T., 2017a. The interaction between the proliferating macroalga Asparagopsis taxiformis and the coral Astroides calycularis induces changes in microbiome and metabolomic fingerprints. Sci. Rep. 7, 1–14. https://doi.org/10.1038/srep42625

Greff, S., Zubia, M., Genta-Jouve, G., Massi, L., Perez, T., Thomas, O.P., 2014. Mahorones, highly brominated cyclopentenones from the red alga Asparagopsis taxiformis. J. Nat. Prod. 77, 1150–1155. https://doi.org/10.1021/np401094h

Greff, S., Zubia, M., Payri, C., Thomas, O.P., Perez, T., 2017b. Chemogeography of the red macroalgae Asparagopsis: metabolomics, bioactivity, and relation to invasiveness. Metabolomics 13, 0. https://doi.org/10.1007/s11306-017-1169-z

Gutow, L., Rahman, M.M., Bartl, K., Saborowski, R., Bartsch, I., Wiencke, C., 2014. Ocean acidification affects growth but not nutritional quality of the seaweed Fucus vesiculosus (Phaeophyceae, Fucales). J. Exp. Mar. Bio. Ecol. 453, 84–90. https://doi.org/10.1016/j.jembe.2014.01.005

Hall-Spencer, J.M., Rodolfo-Metalpa, R., Martin, S., Ransome, E., Fine, M., Turner, S.M., Rowley, S.J., Tedesco, D., Buia, M.C., 2008. Volcanic carbon dioxide vents show ecosystem effects of ocean acidification. Nature 454, 96–99. https://doi.org/10.1038/nature07051

Halsall, T.G., Hills, I.R., 1971. Isolation of heneicosa-1,6,9,12,15,18-hexaene and -1,6,9,12,15-pentaene from the alga Fucus vesiculosus. J. Chem. Soc. D Chem. Commun. 448–449. https://doi.org/10.1039/C29710000448

Hammer, K.M., Pedersen, S.A., Storseth, T.R., 2012. Elevated seawater levels of CO2 change the metabolic fingerprint of tissues and hemolymph from the green shore crab Carcinus maenas. Comp. Biochem. Physiol. - Part D Genomics Proteomics 7, 292–302. https://doi.org/10.1016/j.cbd.2012.06.001

Hoegh-Guldberg, O., 2014. Coral reef sustainability through adaptation: Glimmer of hope or persistent mirage? Curr. Opin. Environ. Sustain. 7, 127–133. https://doi.org/10.1016/j.cosust.2014.01.005

Holbrook, G.P., Beer, S., Spencer, W.E., Reiskind, J.B., Davis, J.S., Bowes, G., 1988. Photosynthesis in marine macroalgae: evidence for carbon limitation. Can. J. Bot. 66, 577–582. https://doi.org/10.1139/b88-083

Holbrook, S.J., Schmitt, R.J., Adam, T.C., Brooks, A.J., 2016. Coral Reef Resilience , Tipping Points and the Strength of Herbivory. Sci. Rep. 6, 1–11. https://doi.org/10.1038/srep35817

Hughes, T.P., 1994. Catastrophes , Phase Shifts , and Large-Scale Degradation of a Caribbean Coral Reef. Science (80-. ). 265, 1547–1552.

Hughes, T.P., Barnes, M.L., Bellwood, D.R., Cinner, J.E., Cumming, G.S., 2017. Coral reefs in the Anthropocene. Nature 546, 82–90. https://doi.org/10.1038/nature22901

Iñiguez, C., Carmona, R., Lorenzo, M.R., Niell, F.X., Wiencke, C., Gordillo, F.J.L., 2016. Increased CO2 modifies the carbon balance and the photosynthetic yield of two common Arctic brown seaweeds: Desmarestia aculeata and Alaria esculenta. Polar Biol. 39, 1979–1991. https://doi.org/10.1007/s00300-015-1724-x

Ivanišević, J., Thomas, O.P., Pedel, L., Penez, N., Ereskovsky, A. V., Culioli, G., Perez, T., 2011. Biochemical trade-offs: Evidence for ecologically linked secondary metabolism of the sponge oscarella balibaloi. PLoS One 6. https://doi.org/10.1371/journal.pone.0028059

Jaramillo, K.B., Reverter, M., Guillen, P.O., McCormack, G., Rodriguez, J., Sinniger, F., Thomas, O.P., 2018. Assessing the Zoantharian Diversity of the Tropical Eastern Pacific through an Integrative Approach. Sci. Rep. 8, 1–15. https://doi.org/10.1038/s41598-018-25086-4

Johnson, M.D., Price, N.N., Smith, J.E., 2014. Contrasting effects of ocean acidification on tropical fleshy and calcareous algae. PeerJ 2, e411. https://doi.org/10.7717/peerj.411

Jompa, J., Mccook, L.J., 2003. Coral – algal competition : macroalgae with different properties have different effects on corals. Mar. Ecol. Prog. Ser. 258, 87–95.

Jompa, J., Mccook, L.J., 2002. The effects of nutrients and herbivory on competition between a hard coral ( Porites cylindrica ) and a brown alga ( Lobophora variegata ). Limnol. Oceanogr. 47, 527–534.

Koch, M., Bowes, G., Ross, C., Zhang, X.H., 2013. Climate change and ocean acidification effects on seagrasses and marine macroalgae. Glob. Chang. Biol. 19, 103–132. https://doi.org/10.1111/j.1365-2486.2012.02791.x

Kooke, R., Keurentjes, J.J.B., 2012. Multi-dimensional regulation of metabolic networks shaping plant development and performance. J. Exp. Bot. 63, 3353–3365. https://doi.org/10.1093/jxb/err373

Kroeker, K.J., Kordas, R.L., Crim, R., Hendriks, I.E., Ramajo, L., Singh, G.S., Duarte, C.M., Gattuso, J.P., 2013. Impacts of ocean acidification on marine organisms: Quantifying sensitivities and interaction with warming. Glob. Chang. Biol. 19, 1884–1896. https://doi.org/10.1111/gcb.12179

Kroeker, K.J., Kordas, R.L., Crim, R.N., Singh, G.G., 2010. Meta-analysis reveals negative yet variable effects of ocean acidification on marine organisms. Ecol. Lett. 13, 1419–1434. https://doi.org/10.1111/j.1461-0248.2010.01518.x

Kumar, A., AbdElgawad, H., Castellano, I., Selim, S., Beemster, G.T.S., Asard, H., Buia, M.C., Palumbo, A., 2018. Effects of ocean acidification on the levels of primary and secondary metabolites in the brown macroalga Sargassum vulgare at different time scales. Sci. Total Environ. 643, 946–956. https://doi.org/10.1016/j.scitotenv.2018.06.176

Kumar, M., Kuzhiumparambil, U., Pernice, M., Jiang, Z., Ralph, P.J., 2016. Metabolomics : an emerging frontier of systems biology in marine macrophytes. Algal Res. 16, 76–92. https://doi.org/10.1016/j.algal.2016.02.033

Ledlie, M.H., Graham, N.A.J., Bythell, J.C., Wilson, S.K., Jennings, S., Polunin, N.V.C., Hardcastle, J., 2007. Phase shifts and the role of herbivory in the resilience of coral reefs. Coral Reefs 26, 641–653. https://doi.org/10.1007/s00338-007-0230-1

Lirman, D., Biber, P., 2000. Seasonal Dynamics of Macroalgal Communities of the Northern Florida Reef Tract 43, 305–314.

López-Legentil, S., Bontemps-Subielos, N., Turon, X., Banaigs, B., 2006. Temporal variation in the production of four secondary metabolites in a colonial ascidian. J. Chem. Ecol. 32, 2079–2084. https://doi.org/10.1007/s10886-006-9148-2

Martí, R., Uriz, M.J., Turon, X., 2004. Seasonal and spatial variation of species toxicity in Mediterranean seaweed communities : correlation to biotic and abiotic factors. Mar. Ecol. Prog. Ser. 282, 73–85.

McCook, L., Jompa, J., Diaz-Pulido, G., 2001. Competition between corals and algae on coral reefs: a review of evidence and mechanisms. Coral Reefs 19, 400–417. https://doi.org/10.1007/s003380000129

Moberg, F., Folke, C., 1999. Ecological goods and services of coral reef ecosystems. Ecol. Econ. 29, 215–233. https://doi.org/10.1016/S0921-8009(99)00009-9

Mumby, P.J., Foster, N.L., Glynn Fahy, E.A., 2005. Patch dynamics of coral reef macroalgae under chronic and acute disturbance. Coral Reefs 24, 681–692. https://doi.org/10.1007/s00338-005-0058-5

Munday, P.L., Cheal, A.J., Dixson, D.L., Rummer, J.L., Fabricius, K.E., 2014. Behavioural impairment in reef fishes caused by ocean acidification at CO 2 seeps. Nat. Clim. Chang. 4, 487–492. https://doi.org/10.1038/NCLIMATE2195

Nugues, M.M., Bak, R.P.M., 2008. Long-term dynamics of the brown macroalga Lobophora variegata on deep reefs in Curaçao. Coral Reefs 27, 389–393. https://doi.org/10.1007/s00338-007-0346-3

Nunes, J., McCoy, S.J., Findlay, H.S., Hopkins, F.E., Kitidies, V., 2016. Two intertidal, non-calcifying macroalgae (Palmaria palmata and Saccharina latissima) show complex and variable responses to short-term CO2 acidificatio. ICES J. Mar. Sci. 73, 887–896.

Porzio, L., Buia, M.C., Lorenti, M., De Maio, A., Arena, C., 2017. Physiological responses of a population of Sargassum vulgare (Phaeophyceae) to high pCO2/low pH: implications for its long-term distribution. Sci. Total Environ. 576, 917–925. https://doi.org/10.1016/j.scitotenv.2016.10.096

Ragazzola, F., Foster, L.C., Form, A., Anderson, P.S.L., Hansteen, T.H., Fietzke, J., 2012. Ocean acidification weakens the structural integrity of coralline algae. Glob. Chang. Biol. 18, 2804–2812. https://doi.org/10.1111/j.1365-2486.2012.02756.x

Rasher, D.B., Hay, M.E., 2014. Competition induces allelopathy but suppresses growth and anti-herbivore defence in a chemically rich seaweed. Proc. R. Soc. B Biol. Sci. 281. https://doi.org/http://dx.doi.org/10.1098/rspb.2013.2615

Rasher, D.B., Hay, M.E., 2010. Chemically rich seaweeds poison corals when not controlled by herbivores. PNAS 107, 9683–9688. https://doi.org/10.1073/pnas.0912095107

Ries, J.B., Cohen, A.L., McCorkle, D.C., 2009. Marine calcifiers exhibit mixed responses to CO2-induced ocean acidification. Geology 37, 1131–1134. https://doi.org/10.1130/G30210A.1

Roggatz, C.C., Lorch, M., Hardege, J.D., Benoit, D.M., 2016. Ocean acidification affects marine chemical communication by changing structure and function of peptide signalling molecules. Glob. Chang. Biol. 22, 3914–3926. https://doi.org/10.1111/gcb.13354

Shannon, P., Markiel, A., Ozier, O., Baliga, N.S., Wang, J.T., Ramage, D., Amin, N., Schwikowski, B., Ideker, T., 2003. Cytoscape : A Software Environment for Integrated Models of Biomolecular Interaction Networks 2498–2504. https://doi.org/10.1101/gr.1239303.metabolite

Slattery, M., Lesser, M.P., 2014. ALLELOPATHY IN THE TROPICAL ALGA LOBOPHORA VARIEGATA ( PHAEOPHYCEAE ): MECHANISTIC BASIS FOR A PHASE SHIFT ON MESOPHOTIC CORAL REEFS ? J. Phycol. 50, 493–505. https://doi.org/10.1111/jpy.12160

Smith, C.A., Maille, G.O., Want, E.J., Qin, C., Trauger, S.A., Brandon, T.R., Custodio, D.E., Abagyan, R., Siuzdak, G., 2005. A Metabolite Mass Spectral Database 27, 747–751.

Smith, C.A., Want, E.J., Maille, G.O., Abagyan, R., Siuzdak, G., O'Maille, G., Abagyan, R., Siuzdak, G., 2006. XCMS: Processing mass spectrometry data for metabolite profiling using nonlinear peak alignment, matching, and identification. Anal. Chem. 78, 779–787. https://doi.org/10.1021/ac051437y

Sogin, E.M., Putnam, H.M., Anderson, P.E., Gates, R.D., 2016. Metabolomic signatures of increases in temperature and ocean acidification from the reef-building coral, Pocillopora damicornis. Metabolomics 12, 1–12. https://doi.org/10.1007/s11306-016-0987-8

Swanson, A.K., Fox, C.H., 2007. Altered kelp (Laminariales) phlorotannins and growth under elevated carbon dioxide and ultraviolet-B treatments can influence associated intertidal food webs. Glob. Chang. Biol. 13, 1696–1709. https://doi.org/10.1111/j.1365-2486.2007.01384.x

Viant, M.R., 2007. Introducing genomics , proteomics and metabolomics in marine ecology Introduction. Mar.

Ecol. Prog. Ser. 332, 247–248. https://doi.org/10.3354/meps332249

Vieira, B.C., 2015. Université Pierre et Marie Curie Lobophora : biotic interactions and diversification Université Pierre et Marie Curie Ghent University genre Lobophora.

Vieira, C., 2015. Lobophora: biotic interactions and diversification.

Vieira, C., Camacho, O., Sun, Z., Fredericq, S., Leliaert, F., Payri, C., De Clerck, O., 2017. Historical biogeography of the highly diverse brown seaweed Lobophora (Dictyotales, Phaeophyceae). Mol. Phylogenet. Evol. 110, 81–92. https://doi.org/10.1016/j.ympev.2017.03.007

Vieira, C., D'hondt, S., De Clerck, O., Payri, C.E., 2014. Toward an inordinate fondness for stars, beetles and Lobophora? Species diversity of the genus Lobophora (Dictyotales, Phaeophyceae) in New Caledonia. J. Phycol. 50, 1101–1119. https://doi.org/10.1111/jpy.12243

Vieira, C., Thomas, O.P., Culioli, G., Genta-Jouve, G., Houlbreque, F., Gaubert, J., De Clerck, O., Payri, C.E., 2016. Allelopathic interactions between the brown algal genus Lobophora (Dictyotales, Phaeophyceae) and scleractinian corals. Sci. Rep. 6, 18637. https://doi.org/10.1038/srep18637

Wang, M., Carver, J.J., Phelan, L.M., Sanchez, L.M., Garg, N., Al, E., 2016. Sharing and community curation of mass spectrometry data with Global Natural Products Social Molecular Networking. Nat. Biotechnol. 34. https://doi.org/10.1038/nbt.3597

Webster, N.S., Uthicke, S., Botté, E.S., Flores, F., Negri, A.P., 2013. Ocean acidification reduces induction of coral settlement by crustose coralline algae. Glob. Chang. Biol. 19, 303–315. https://doi.org/10.1111/gcb.12008

Wei, L., Wang, Q., Ning, X., Mu, C., Wang, C., Cao, R., Wu, H., Cong, M., Li, F., Ji, C., Zhao, J., 2015. Combined metabolome and proteome analysis of the mantle tissue from Pacific oyster Crassostrea gigas exposed to elevated pCO<inf>2</inf>. Comp. Biochem. Physiol. - Part D Genomics Proteomics 13, 16–23. https://doi.org/10.1016/j.cbd.2014.12.001

Xu, Z., Gao, G., Xu, J., Wu, H., 2017. Physiological response of a golden tide alga ( Sargassum muticum ) to the interaction of ocean acidification and phosphorus enrichment. Biogeosciences 14, 671–681. https://doi.org/10.5194/bg-14-671-2017

Yamori, W., Hikosaka, K., Way, D.A., 2014. Temperature response of photosynthesis in C3, C4, and CAM plants: Temperature acclimation and temperature adaptation. Photosynth. Res. 119, 101–117. https://doi.org/10.1007/s11120-013-9874-6

Youngblood, W.W., Blumer, M., 1973. Alkanes and alkenes in marine benthic algae. Mar. Biol. 21, 163–172. https://doi.org/10.1007/BF00355246

**Figures and tables captions**

**Figure 1**. (a) Powered Partial Least-Squares-Discriminant Analysis (PPLS-DA) score plots of the methanol extracts of *Lobophora rosacea* metabolome from the control (Ricaudy) and low pH (Bouraké) sites, and (b) PPLS-DA loadings (threshold 0.8, see tables 1a and S2 for details about the metabolites). Metabolites in blue refer to Fig. 3 and have been annotated with the help of the molecular network. Compounds in grey were not considered for marker selection. CER = classification error rate with p-value after double cross-model validation.

**Figure 2**. (a) Powered Partial Least-Squares-Discriminant Analysis (PPLS-DA) score plots of *Lobophora rosacea* metabolome analyzed by LC-MS in control and low pH treatments at $t_0$ and $t_{14}$. CER = classification error rate with p-value after double cross-model validation; (b) PPLS-DA loadings (threshold 0.8, see tables 1 and S3 for details about the metabolites). Metabolites in blue refer to Fig. 3 and have been annotated with the help of the molecular network. Compounds in grey were not considered for chemomarker selection.

**Figure 3**. Cluster of the molecular network built in GNPS showing the 10 chemomarkers linked to pH conditions (in blue) that were identified from the *in-situ* (Fig. 1b) and *ex-situ* samples (Fig. 2b). Chemical formulas are displayed for lobophorenols. Red boxes indicate common biomarkers between *ex* situ $t_0$ samples and *in situ* samples (cf. Fig. 5). Ions were detected as $[M+NH_4^+]$, $[M+H^+]$ or $[M+Na^+]$ (see Table 1 for details) but only molecular formulas are indicated in the network for clarity and coherence.

**Figure 4**. Box plots of the chemomarkers linked to seawater pH conditions (control pH: Ricaudy, low pH: Bouraké) present in the cluster of the molecular network (Fig. 3, in blue). The two markers in common between *in situ* and *ex situ* $t_0$ samples are indicated. Ion intensities of chemomarkers are expressed as mean normalized intensities ± SD (log-transformed data, n=8 for *in situ* samples, n=3 for *ex situ* $t_0$ samples). Differences between ion intensities for control vs low pH conditions were tested with Mann-Whitney tests. **: $p < 0.001$.

**Figure 5**. Venn diagram of the chemomarkers of pH conditions (selected on PPLS-DA loadings with threshold = 0.8) identified in *in situ* and *ex situ* samples. Boxes list the common chemomarkers between *in situ* and *ex* situ ($t_0$ and $t_{14}$) samples: red = lower quantities in low pH conditions, yellow = higher quantities in low pH conditions. * indicates chemomarkers present in the cluster, cf. Fig. 3.

**Table 1**. (a) *Lobophora rosacea* chemomarkers of pH conditions present in the cluster of the molecular network (Fig. 3) and (b) chemomarkers in common between *in situ* and *ex situ* samples (identified with the Venn diagram Fig. 5). For each feature: M = nominal mass, T = retention time.

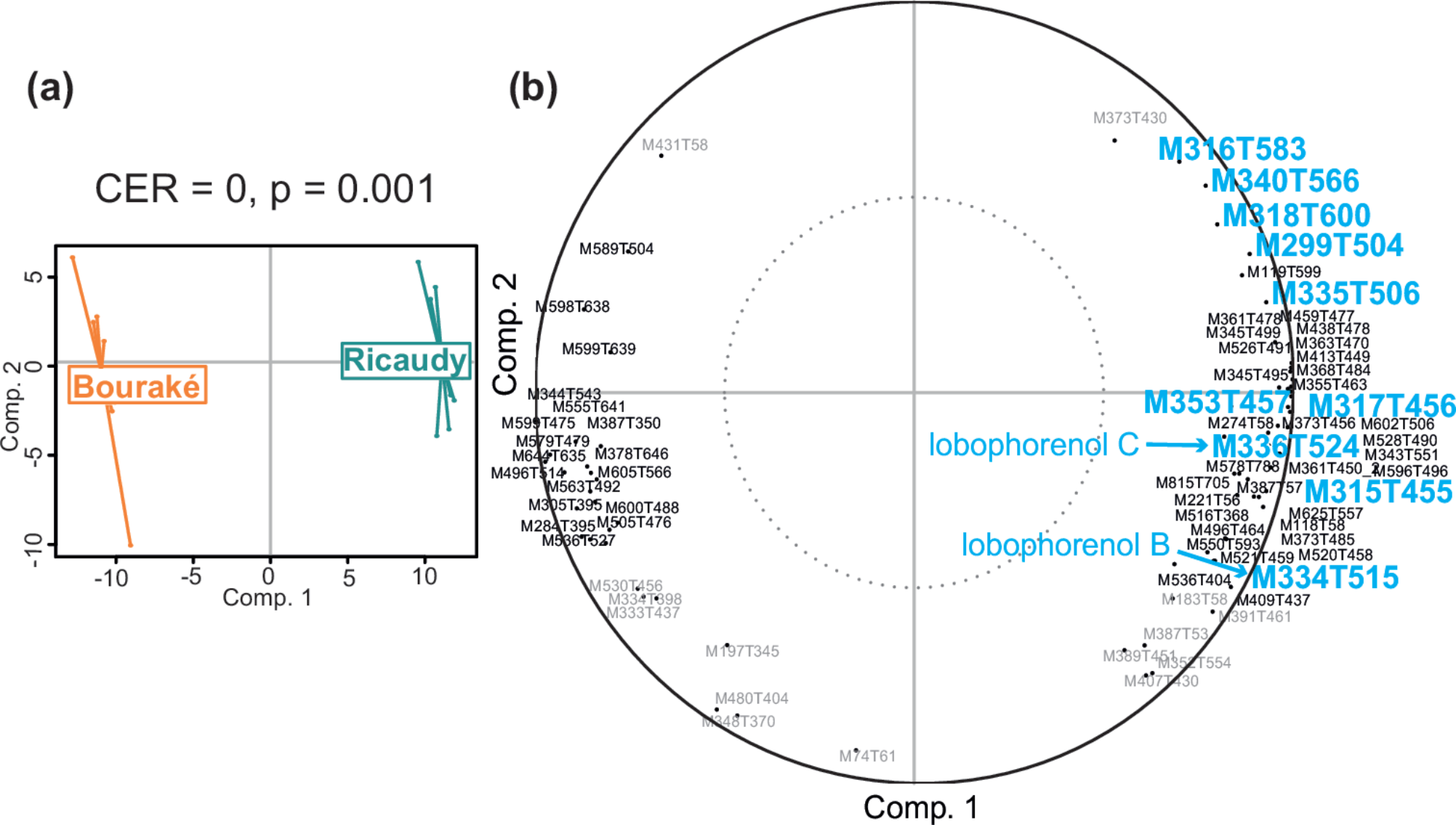
(a)
CER = 0, p = 0.001
Bouraké
Ricaudy
Comp. 2
Comp. 1
5
0
-5
-10
-10
-5
0
5
10
(b)
Comp. 2
Comp. 1
M373T430
M431T58
M316T583
M340T566
M318T600
M299T504
M119T599
M335T506
M589T504
M598T638
M599T639
M344T543
M555T641
M599T475
M387T350
M579T479
M644T635
M378T646
M496T514
M605T566
M563T492
M305T395
M600T488
M284T395
M505T476
M536T527
M530T456
M334T398
M333T437
M197T345
M480T404
M348T370
M74T61
M361T478
M459T477
M345T499
M438T478
M526T491
M363T470
M413T449
M345T495
M368T484
M355T463
M353T457
M317T456
M274T58
M373T456
M602T506
Iobophorenol C
M336T524
M528T490
M343T551
M578T788
M361T450_2
M596T496
M815T705
M387T57
M315T455
M221T56
M516T368
M625T557
M496T464
M118T58
Iobophorenol B
M550T593
M373T485
M521T459
M520T458
M536T404
M334T515
M183T58
M409T437
M391T461
M387T53
M389T451
M352T554
M407T430

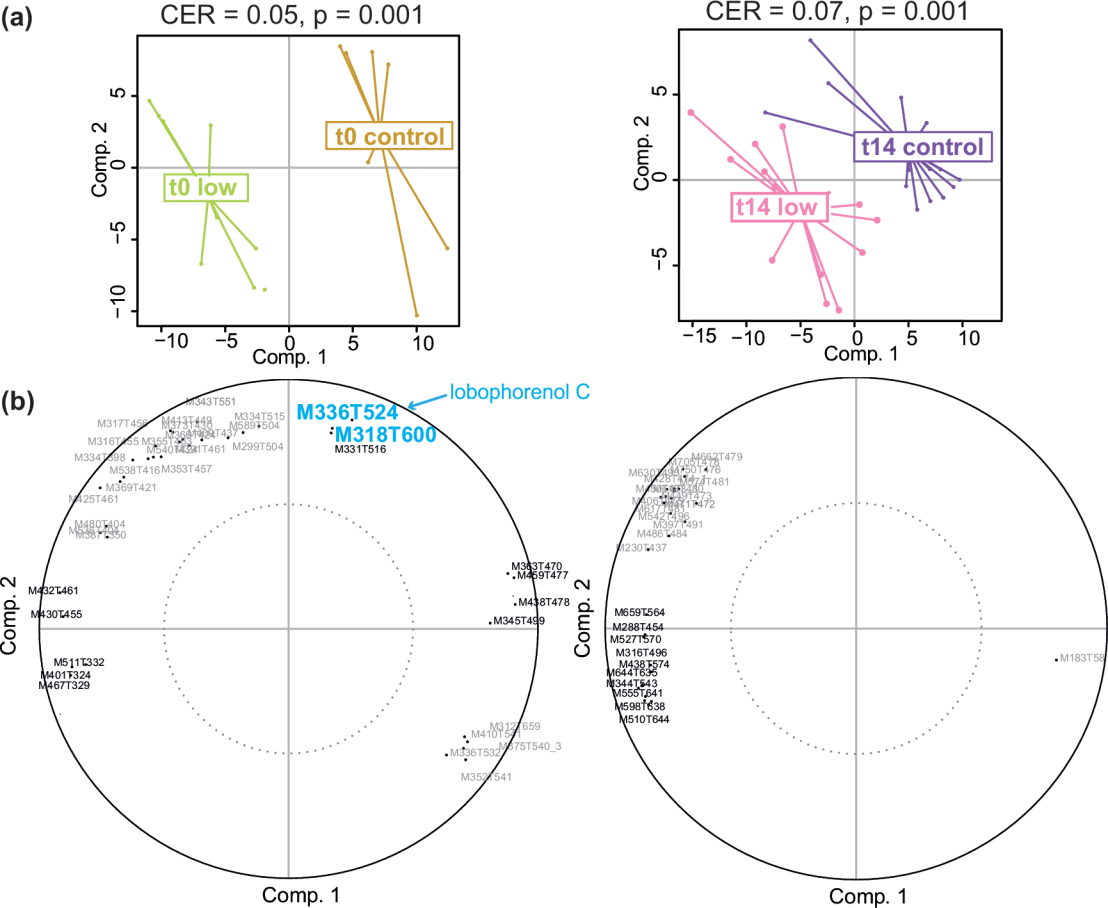
(a)
CER = 0.05, p = 0.001
t0 control
t0 low
Comp. 2
Comp. 1
CER = 0.07, p = 0.001
t14 control
t14 low
Comp. 2
Comp. 1
(b)
lobophorenol C
M336T524
M318T600
M331T516
M343T551
M317T466
M334T515
M689T504
M316T435
M299T504
M334T498
M538T416
M353T457
M369T421
M325T461
M480T404
M363T470
M459T477
M438T478
M345T499
M432T461
M430T455
M511T332
M401T324
M467T329
M312T659
M410T651
M375T540_3
M336T532
M353T541
Comp. 2
Comp. 1
M662T479
M659T564
M288T454
M527T570
M316T496
M438T574
M644T635
M344T643
M555T641
M598T638
M510T644
M183T58
Comp. 2
Comp. 1

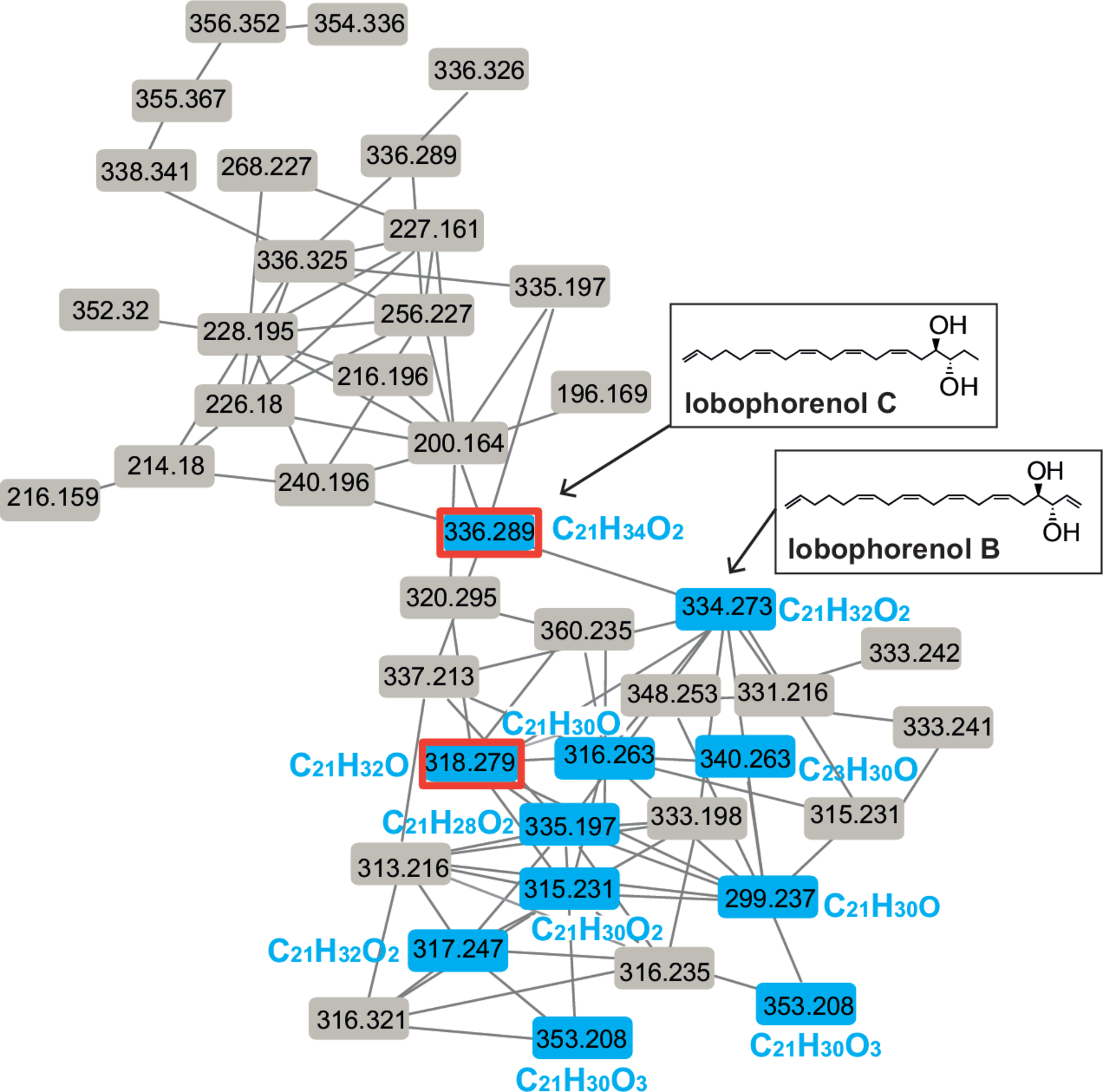
356.352
354.336
336.326
355.367
336.289
338.341
268.227
227.161
336.325
335.197
352.32
256.227
228.195
216.196
196.169
226.18
200.164
214.18
240.196
216.159
336.289
C21H34O2
lobophorenol C
OH
OH
lobophorenol B
OH
OH
320.295
334.273
C21H32O2
360.235
333.242
337.213
348.253
331.216
C21H30O
333.241
C21H32O
318.279
316.263
340.263
C23H30O
315.231
C21H28O2
335.197
333.198
313.216
315.231
299.237
C21H30O
C21H30O2
C21H32O2
317.247
316.235
353.208
316.321
353.208
C21H30O3
C21H30O3

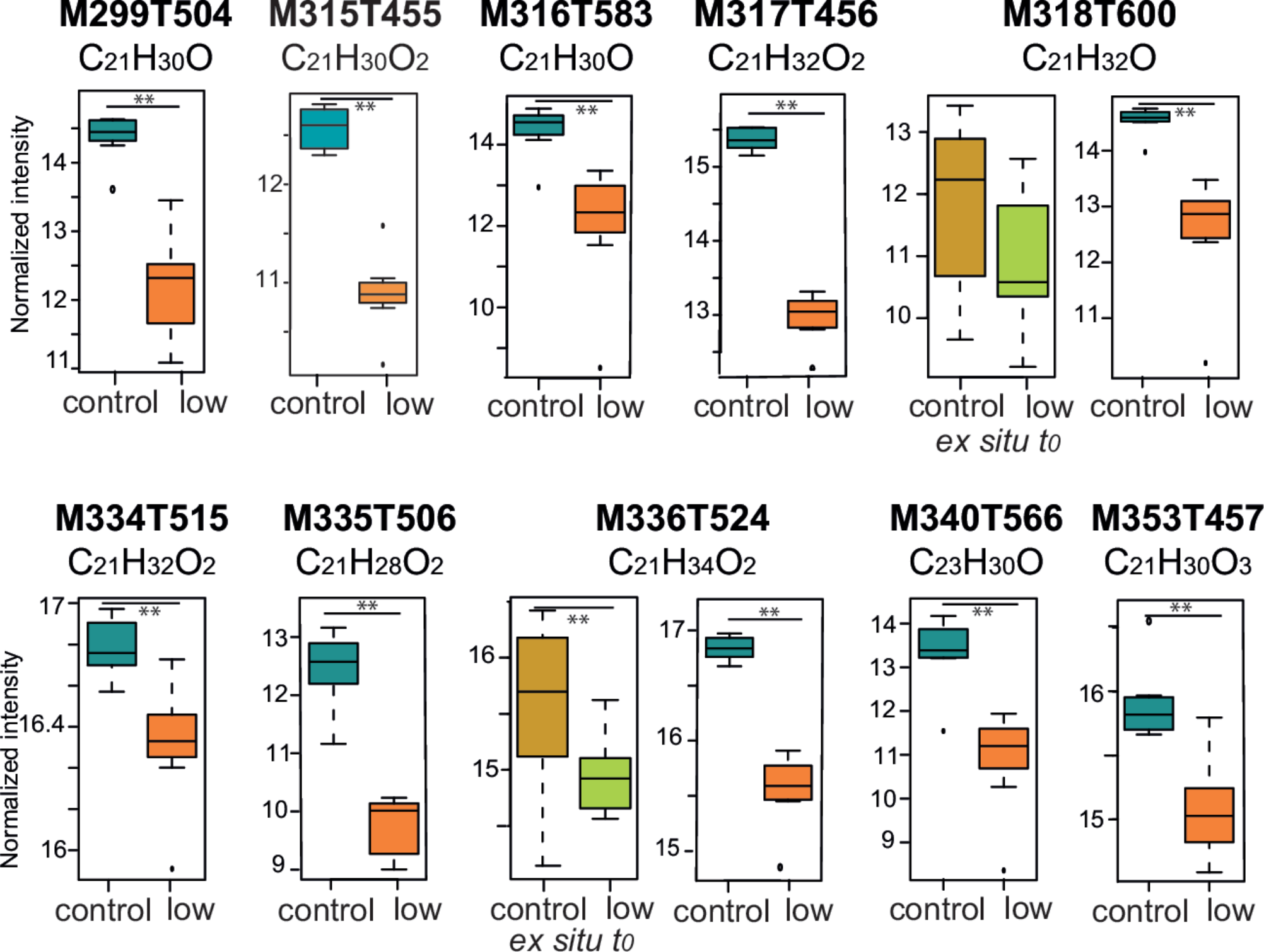
M299T504
C21H30O
M315T455
C21H30O2
M316T583
C21H30O
M317T456
C21H32O2
M318T600
C21H32O
Normalized intensity
control low
ex situ to
M334T515
C21H32O2
M335T506
C21H28O2
M336T524
C21H34O2
M340T566
C23H30O
M353T457
C21H30O3
Normalized intensity
control low
ex situ to

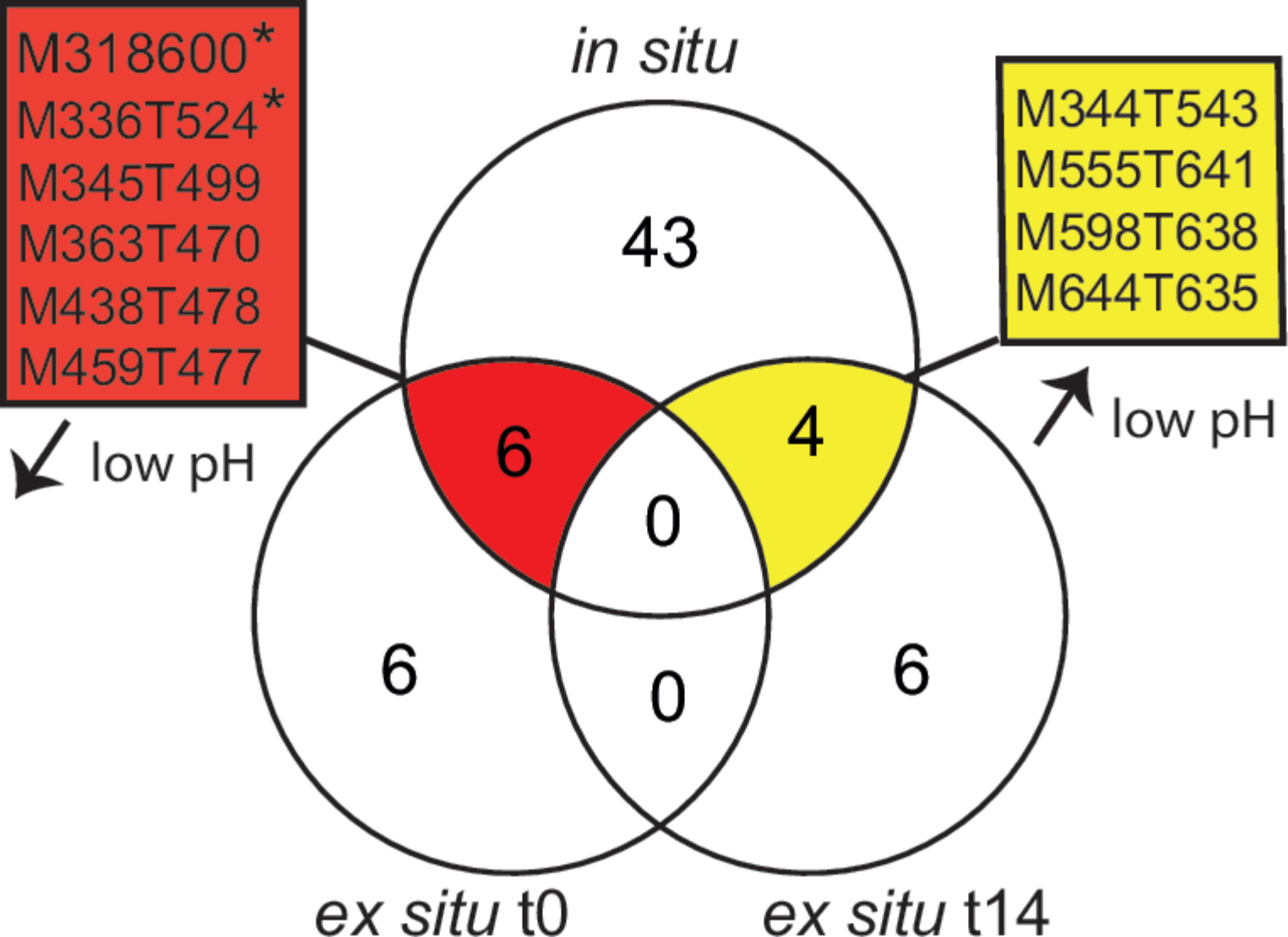
M318600*
M336T524*
M345T499
M363T470
M438T478
M459T477
low pH
in situ
43
6
4
0
6
0
6
ex situ t0
ex situ t14
M344T543
M555T641
M598T638
M644T635
low pH

**Table 1**. (a) *Lobophora rosacea* chemomarkers of pH conditions present in the cluster of the molecular network (Fig. 3) and (b) chemomarkers in common between *in situ* and *ex situ* samples (identified with the Venn diagram Fig. 5). For each feature: M = nominal mass, T = retention time.

| **Features** | ***m/z*** | **Molecular formula** | **Error (ppm)** | **Ion** | **Annotation** | **Chemomarker intensity compared to control conditions** |
|---|---|---|---|---|---|---|
| *a/ chemomarkers of pH conditions found in the cluster of the molecular network (Fig. 3) (* including two markers in common between in situ and ex situ $t_0$ samples)* | | | | | | |
| M299T504 | 299.2367 | $C_{21}H_{30}O$ | -2.7 | $[M+H]^+$ | | ↓ |
| M315T455 | 315.2319 | $C_{21}H_{30}O_2$ | -0.1 | $[M+H]^+$ | | ↓ |
| M316T583 | 316.2634 | $C_{21}H_{30}O$ | 1.5 | $[M+NH_4]^+$ | | ↓ |
| M317T456 | 317.2474 | $C_{21}H_{32}O_2$ | 0.2 | $[M+H]^+$ | | ↓ |
| M318T600* | 318.2786 | $C_{21}H_{32}O$ | -0.9 | $[M+NH_4]^+$ | | ↓ |
| M334T515 | 334.2740 | $C_{21}H_{32}O_2$ | 0 | $[M+NH_4]^+$ | Lobophorenol B | ↓ |
| M335T506 | 335.1971 | $C_{21}H_{28}O_2$ | 6.1 | $[M+Na]^+$ | | ↓ |
| M336T524* | 336.2896 | $C_{21}H_{34}O_2$ | 0.4 | $[M+NH_4]^+$ | Lobophorenol C | ↓ |
| M340T566 | 340.2634 | $C_{23}H_{30}O$ | -0.8 | $[M+NH_4]^+$ | | ↓ |
| M353T457 | 353.2086 | $C_{21}H_{30}O_3$ | 0.1 | $[M+Na]^+$ | | ↓ |
| *b/ chemomarkers of pH conditions in common between in situ and ex situ samples* | | | | | | |
| *In situ / ex situ $t_0$* | | | | | | |
| M345T499 | 345.2422 | $C_{22}H_{32}O_3$ | -1 | $[M+H]^+$ | | ↓ |
| M363T470 | 363.2530 | $C_{22}H_{34}O_4$ | 2.2 | $[M+H]^+$ | | ↓ |
| M438T478 | 438.2850 | $C_{24}H_{36}O_6$ | 0.1 | $[M+NH_4]^+$ | | ↓ |
| M459T477 | 459.2166 | $C_{29}H_{30}O_5$ | 3.4 | $[M+H]^+$ | | ↓ |
| *In situ / ex situ $t_{14}$* | | | | | | |
| M344T543 | 344.3159 | $C_{20}H_{38}O_3$ | -2.9 | $[M+NH_4]^+$ | | ↑ |
| M555T641 | 555.4660 | - | - | - | | ↑ |
| M598T638 | 598.4889 | - | - | - | | ↑ |
| M644T635 | 643.5192 | - | - | - | | ↑ |

*In situ*

**Long-term effect of ocean acidification**

*Natural acidic system*

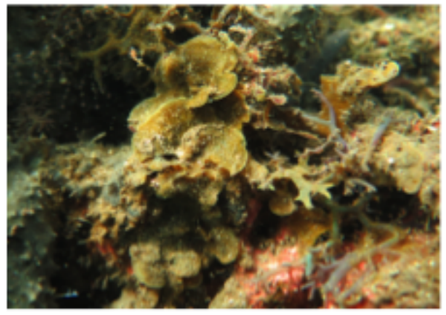

≠ metabolomes?

*Control pH site*

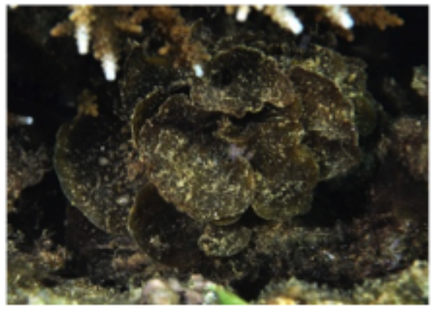

*Ex situ*

**Short-term effect of ocean acidification**

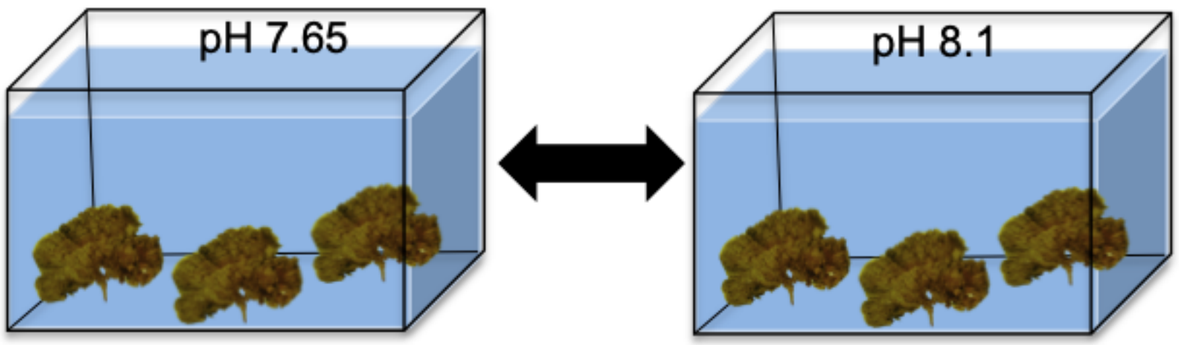


**UHPLC-qTOF analyses**

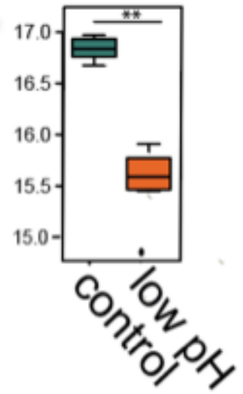


**Molecular network**

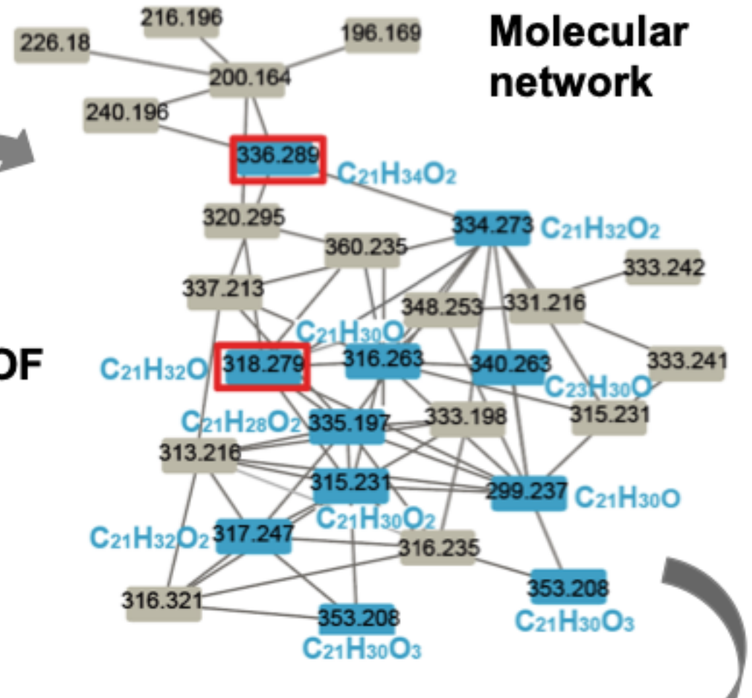


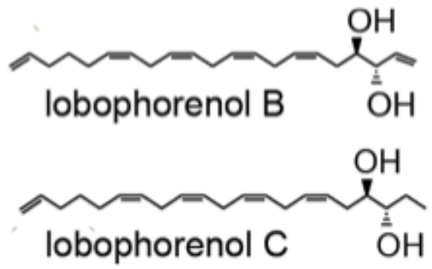


**Chemomarkers of pH condition**